ISBN: 978-3-95450-208-0 doi:10.18429/JACoW-IPAC2019-TUPRB052

# THE MINI-PERIOD PERMANENT MAGNET STAGGERED UNDULATOR FOR COMPACT X-RAY FREE ELECTRON LASER *

L. G. Yan, D. R. Deng, J. X. Wang †
Institute of Applied Electronic, China Academy of Engineering and Physics, Mianyang, China

*Abstract*

Miniaturization of X-ray free electron laser requires reduction of undulator period length. In this proceeding, a mini-period permanent magnet staggered undulator was proposed, which is free of superconducting solenoid and thus has advantages of easy-manufacture and low-cost. After optimization, it can generate periodic field of peak field 0.71 T with period length 10 mm and pole gap 2 mm, which has been verified on a prototype. Combined with X-band linac, the length of 1 nm XFEL facility using the permanent magnet staggered undulator can be confined within 44 m.

## INTRODUCTION

In recent years, X-ray free electron laser (XFEL) became operational and have opened new exciting opportunities for scientific applications. Undulator plays a key role in XFEL and radiation wavelength $\lambda_r$ from undulator is determined by Eq. (1), in which $\lambda_u$, $\gamma$, and $K$ are undulator period length, relativistic factor and undulator parameter, respectively. It can be seen shortening undulator period length can reduce electron beam energy for a given wavelength, which helps to miniaturize XFEL and reduce the construction and maintenance costs. To pursue undulator with shorter period length, in-vacuum undulator, cryogenic undulator, superconducting undulator, etc. were proposed and have been studied extensively [1]. But realized period length is still larger than 10 mm now. A solenoid-derived staggered undulator (SSU) was proposed by A. H. Ho, and period length can be reduced below 10 mm thanks to its simple magnetic structure [2]. SSU has attracted widespread interest and been also developed by many other researchers [3, 4]. But in all of their schemes, a superconducting solenoid was used, which meant high-cost and difficulty in manufacture and maintenance. In this proceeding, the superconducting solenoid was replaced by a permanent magnet circuit and a mini-period permanent magnet staggered undulator (PMSU) was proposed. The magnetic structure was designed and optimized, and a prototype was fabricated and measured. We also explored the possibility of adopting PMSU in a compact XFEL.

$$\lambda_r = \frac{\lambda_u}{2\gamma^2}\left(1 + \frac{1}{2}K^2\right) \tag{1}$$

## MAGNETIC STRUCTURE

The proposed undulator PMSU were developed based on the existing SSU [2]. The magnetic structure of PMSU in Radia is shown in Fig. 1. Unlike SSU using superconducting solenoid, PMSU has two longitudinally-magnetized permanent magnet blocks to generate a longitudinal field in their gap. Like SSU, there is a staggered array of high-permeability poles situated inside the gap of permanent magnet blocks to deflect the longitudinal field, thereby providing a transverse periodic field. Two edges of rectangle permanent magnet blocks must be chamfered properly to reduce demagnetizing field and flatten distribution of longitudinal field, which is crucial to suppress the peak-to-peak error of periodic field. In this proceeding, the materials of permanent magnet block and pole block are NdFeB and DT4, respectively, and one can choose other permanent magnetic material or soft magnetic material for a certain application situation. Due to free of superconducting solenoid, PMSU has the advantages of simple structure, easy manufacture, convenient maintenance and low cost.

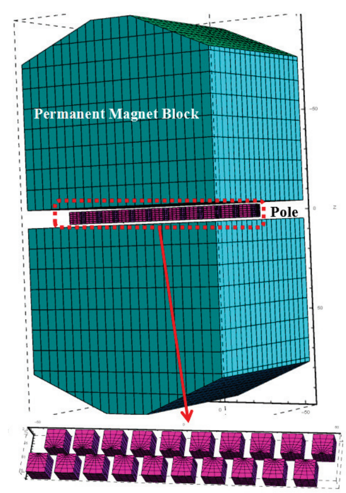


Figure 1: Magnetic structure of PMSU in Radia.

## OPTIMIZATION AND MEASUREMENT

### *Optimization*

Genetic Algorithm (GA) is one of the most excellent methods to search the optimal solution to a problem, which has been applied to solve various problems. In order to maximize peak field and minimize peak-to-peak error of PMSU's periodic field, multi-objective GA was used to optimize parameters of magnetic structure with period length 10 mm, pole gap 2 mm and period number 10. Peak field $B_{rms}$ and peak-to-peak error $\frac{\Delta B}{B}_{rms}$ were set as objective variables. In order to simplify the problem, the weight coefficient transformation method was used to transform multi-objective op-

* Work supported by National Natural Science Foundation of China under grant of 11505174, 11505173 and 11605190.
† jianxinwang1026@163.com

ISBN: 978-3-95450-208-0　doi:10.18429/JACoW-IPAC2019-TUPRB052

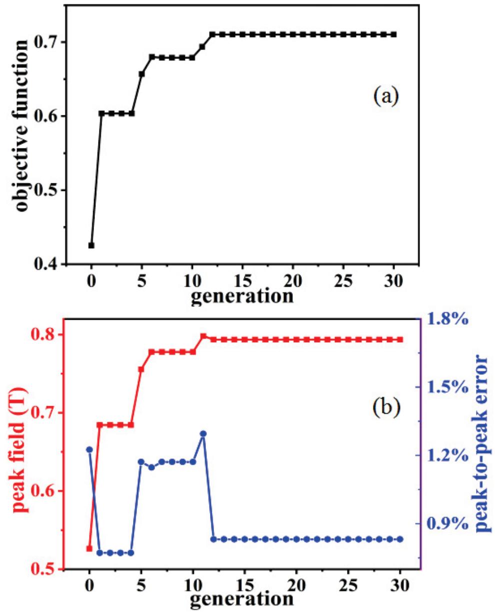


Figure 2: Evolution process: (a) objective function, (b) peak field and peak-to-peak error.

Table 1: Parameters of PMSU After Optimization

| Parameters | | Values |
|---|---|---|
| Period length | | 10 mm |
| Period number | | 10 |
| Pole gap | | 2 mm |
| Pole block | Length | 6.8 mm |
| | Width | 6.6 mm |
| | Height | 6.1 mm |
| | Material | DT4 |
| Permanent magnet block | Length | 108 mm |
| | Width | 86 mm |
| | Height | 90 mm |
| | Chamfer | 18×42.5 mm |
| | Material | NdFeB |

timization problem into single-objective optimization problem. In addition, the two objective variables should have the same priority in the optimization process. Because their numerical values were not in the same range, so they were transformed into roughly same range by appropriate weight coefficients and then the objective function is like Eq. (2). Figure 2 shows the evolution of objective function and two objective variables. Results keep stable after the 12th generation, which means evolution has finished. Table 1 lists the parameters of PMSU after optimization.

$$T[B(z)] = B_{rms} - (4.5 * (\frac{\Delta B}{B})_{rms} + 0.045) \quad (2)$$

### *Measurement*

To verify the above optimization results, a prototype of PMSU was fabricated as shown in Fig. 3, and then measured

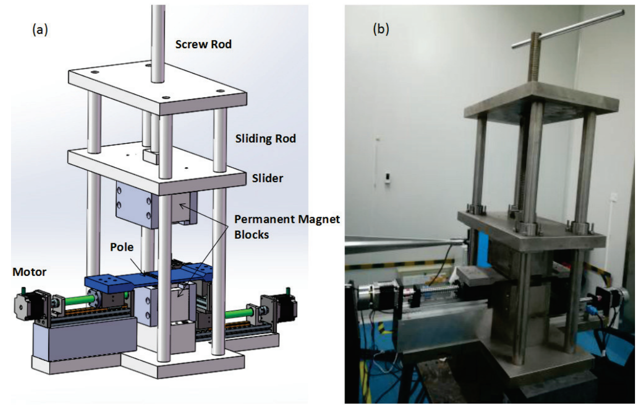


Figure 3: Prototype of PMSU: (a) 3D drawing, (b) physical object

using a magnetic measurement bench. Figure 4 shows longitudinal distribution of periodic field by calculation and measurement. The calculation and measurement results of peak field are 0.79 T and 0.71 T, respectively. There is a 10.7% difference, which may be mainly due to fabricating errors of prototype.

The longitudinal distribution of periodic field under the pole gaps of 2 ~ 6 mm was also calculated and measured. The curve of peak field vs pole gap is shown in Fig. 5. There is an exponential relationship between peak field and pole gap like conventional undulator, which can be used to adjust periodic field of PMSU.

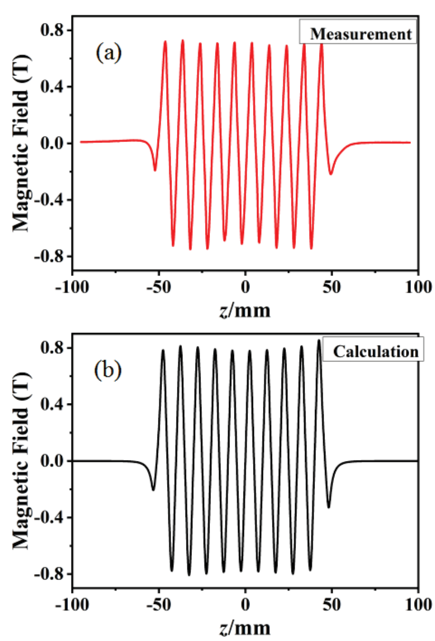


Figure 4: Distribution of periodic field: (a) calculation, (b) measurement

ISBN: 978-3-95450-208-0 doi:10.18429/JACoW-IPAC2019-TUPRB052

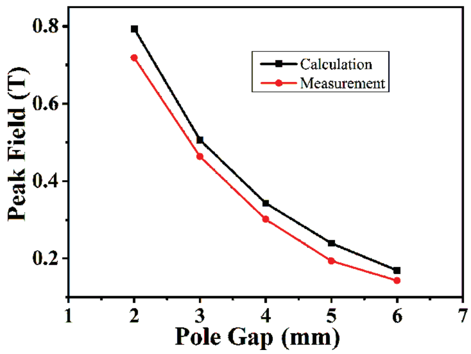


Figure 5: Peak field VS pole gap.

## COMPACT XFEL

In the following, a concrete example of compact XFEL (called C-XFEL in this proceeding) lasing with SASE (Self-Amplified Spontaneous Emission) scheme at 1 nm is shown to demonstrate the effect of PMSU on reducing the scale of XFEL. C-XFEL used PMSU with above-obtained parameters of period length 10 mm and peak field 0.71 T. Table 2 shows the PMSU's parameters of electron beam, undulator line and radiation.

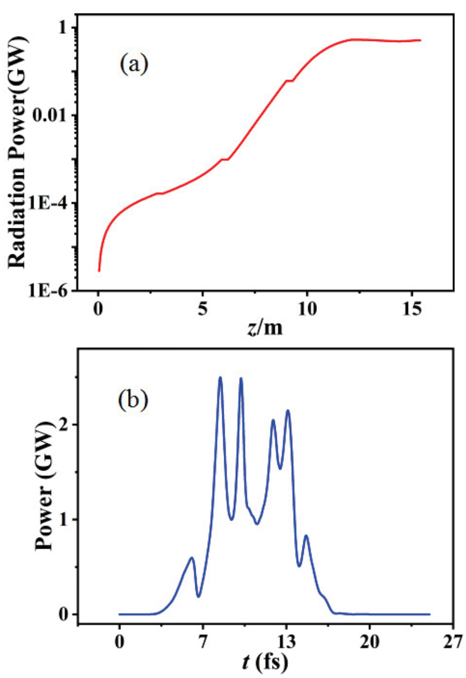


Figure 6: (a) Power gain along undulator line, (b) power temporal profile of radiation pulse at $z$ = 12.3 m.

The electron energy was estimated about 1.26 GeV. Optimum matching of electron to light can be achieved if the condition Eq. (3) is met, where $\varepsilon_N$ is normalized emittance. That means $\varepsilon_N \leq 0.2$ mm mrad, and such low emittance only can be achieved with low charge. Therefore, C-XFEL will run on low charge operation mode and beam charge is 20 pC.

$$\varepsilon_N \leq \gamma \frac{\lambda_r}{4\pi} \tag{3}$$

Undulator line consists totally 5 undulator segments and has external intersperse FODO focusing lattice, so that the average betatron function is about 6.2 m. The radiation characteristics was simulated using GENESIS1.3 code in time-dependent mode. Unlike conventional Halbach undulator PMSU has extra longitudinal magnetic field, so a appropriate longitudinal field was superposed on periodic field during simulation. The radiation power is saturated at $z$ = 12.3 m, as shown in Fig. 6(a). The power temporal profile of radiation pulse at $z$ = 12.3 m is shown in Fig. 6(b) and one can see peak power is about 2.5 GW.

In C-XFEL, X-band linac was assumed to accelerate electron, which can produce an effective average real estate gradient of 60 MV/m when components such as quadrupoles were included [5]. 1.26 GeV X-band linac has a length of about 21 m and the total length of injector and chicane is assumed 8 m, so the entire length of C-XFEL can be confined within 44 m (8 m + 21 m + 15.4 m).

Table 2: Parameters of C-XFEL

| | Parameters | Values |
|---|---|---|
| Electron Beam | Energy | 1.26 GeV |
| | Charge | 20 pC |
| | Beam Length | 5 fs |
| | Emittance, $\varepsilon_N$ | 0.2 mm mrad |
| | Spread | 0.0001 |
| | Peak Current | 1195 A |
| Undulator Line | Pole Gap | 2 mm |
| | Period Length | 10 mm |
| | Peak Field | 0.71 T |
| | Undulator Length | 2.8 m |
| | Segment Interval | 0.3 m |
| | Number of Segments | 5 |
| | Lattice | FODO |
| | Average Betatron Function | 6.2 m |
| Radiation | Wavelength | 1 nm |
| | Peak Power | 2.5 GW |
| | Saturation Length | 12.3 m |
| | Pierce Parameter | 0.0092 |

## CONCLUSION

In this proceeding, PMSU was proposed to reduce the scale of XFEL. PMSU is free of superconducting solenoid, therefore it has advantages of simple structure, easy fabrication, convenient maintenance and low cost. With period length 10 mm and pole gap 2 mm, a peak field of 0.71 T was obtained and verified on a prototype. If the electron is accelerated by a X-band linac with effective gradient 60 MV/m, the length of 1 nm XFEL using PMSU is estimated with in about 44 m. It is truly compacter than other XFEL facilities with radiation wavelength in the same range.

ISBN: 978-3-95450-208-0 doi:10.18429/JACoW-IPAC2019-TUPRB052



## REFERENCES

[1] J. Bahrdt and E. Gluskin, "Cryogenic permanent magnet and superconducting undulators," *Nuclear Instruments and Methods in Physics Research Section A: Accelerators, Spectrometers, Detectors and Associated Equipment*, vol. 907, pp. 149–168, 2018.

[2] A. H. Ho, R. H. Pantell, J. Feinstein, and Y. C. Huang, "A solenoid-derived wiggler," *IEEE Journal of Quantum Electronics*, vol. 27, pp. 2650–2655, 1991.

[3] R. Kinjo *et al.*, "Demonstration of a high-field short-period undulator using bulk high-temperature superconductor," *Applied Physics Express*, vol. 6, 2013.

[4] L. Chen and Q. Jia, "A new modified staggered array undulator," *Nuclear Instruments and Methods in Physics Research Section A: Accelerators, Spectrometers, Detectors and Associated Equipment*, vol. 927, pp. 419–423, 2019.

[5] Y. P. Sun, C. Adolphsen, C. Limborg-Deprey, T. Raubenheimer, and J. H. Wu, "Low-charge, hard x-ray free electron laser driven with an x-band injector and accelerator," *Physical Review Special Topics-Accelerators and Beams*, vol. 15, no. 3, 2012.